

LIDAR OBSERVATIONS OF FINE-SCALE ATMOSPHERIC GRAVITY WAVES IN THE NOCTURNAL BOUNDARY LAYER ABOVE AN ORCHARD CANOPY

Elizabeth R. Jachens and Shane D. Mayor

Departments of Geosciences and Physics

California State University Chico, 400 West First St., Chico, CA 95929, USA

ABSTRACT

Fifty-two episodes of micrometeorological gravity wave activity were identified in data collected with the Raman-shifted Eye-safe Aerosol Lidar (REAL) near Dixon, California, during a nearly continuous 3-month period of observation. The waves, with wavelengths ranging from 40 m to 100 m, appear in horizontal cross-sectional elastic backscatter images of the atmospheric roughness sub-layer between 10 m and 30 m AGL. All of the episodes occur at night when the atmosphere tends toward stability. Time-series data from in situ sensors mounted to a tower that intersected the lidar scans at 1.6 km range reveal oscillations in all three wind velocity components and in some cases the temperature and relative humidity traces. We hypothesize that the lidar can reveal these waves because of the existence of vertical gradients of aerosol backscatter and the oscillating vertical component of air motion in the wave train that displace the backscatter gradients vertically.

1. INTRODUCTION

The atmospheric boundary layer (ABL) is that part of the troposphere that is directly influenced by the presence of the earth's surface, and responds to surface forcings with a timescale of about an hour or less [1]. During the daytime and over land, the ABL is usually hundreds of meters to a kilometer or more in depth and is characterized by large eddies that mix heat, moisture, trace gases, pollutants, and momentum very effectively in both the horizontal and vertical dimensions. At night, radiant energy from the sun is no longer available to warm the surface and drive convective thermals. As a result, the nocturnal ABL tends towards static stability supporting stratification, vertical wind shear, gravity wave activity, and intermittent turbulence confined to shallow layers. This complex nocturnal flow regime presents significant observational and modeling challenges. In this paper, we report on new lidar observations of what appear to be fine-scale waves within 20 m of the top of an orchard canopy.

2. PREVIOUS STUDIES

Observations in the form of time-series and limited amounts of spatial sampling from previous studies have revealed wave-like oscillations at night above forest canopies [2; 3; 4; 5; 6]. The oscillations in the time-series data from previous studies typically resemble more of a sawtooth pattern than a pure sinusoidal wave. Ramp-like steady increases of in situ variables are typically followed

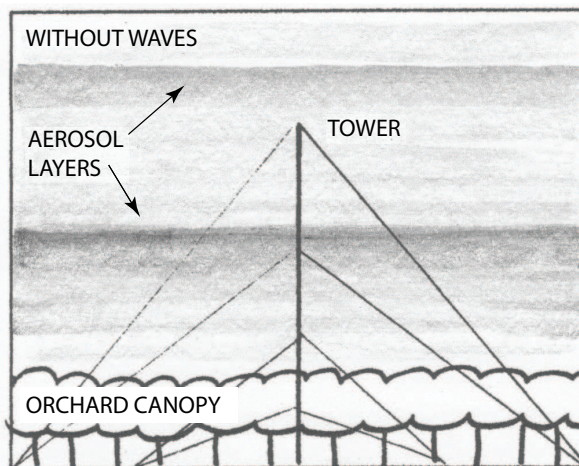


Figure 1: Sketch of a vertical cross-section of the lower atmosphere (from the surface to about 40 m AGL) that may occur at night during quiescent conditions. Stable stratification and weak flow result in the formation of vertical gradients of aerosol backscatter that are horizontally invariant.

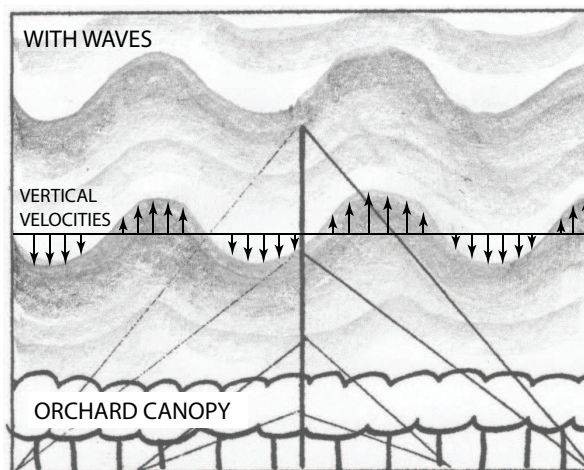


Figure 2: Sketch of a vertical cross-section of the lower atmosphere showing how the vertical wind component w caused by gravity waves (as observed in the bottom traces in Figs. 4, 6, and 8) can vertically displace the horizontal aerosol strata shown in Fig. 1 and enable the elastic backscatter lidar to observe the wave structure in a near-horizontal plane as shown in Figs. 3, 5, and 7. The horizontal line is the approximate altitude of the horizontal lidar scans in Figs. 3, 5, and 7.

by steep decreases. A distinction between ramps and wave oscillations, and the causes of each, has not been made [4]. The most recognized explanation for the cause of the oscillations is shear instability. Lee [5] describes the process of creating the structures when the wind speed shear is at a maximum causing the layers to curl into each other (i.e., Kelvin-Helmholtz billows). An alternative hypothesis of the cause of the observed waves is simple vertical harmonic motion as the result of the displacement of air parcels in a statically stable atmosphere [6].

3. CHATS

The Canopy Horizontal Array Turbulence Study (CHATS) [7] took place in Dixon, California, from 15 March through 11 June 2007. The 3 month field project was aimed at gathering microscale meteorological data in and near the top of a forest canopy. A large walnut orchard (mean tree top height of 10 m) was selected for an experimental site because of its large area in flat terrain and the uniform characteristics of the trees such as their spacing and height. The NCAR ISFF 30-m vertical tower (VT) was installed in the orchard. The Raman-shifted Eye-safe Aerosol Lidar (REAL) [8] was located 1.61 km north of the VT and collected data nearly continuously in the broad area surrounding the VT and the orchard. The REAL provides two-dimensional spatial images of aerosol backscatter intensity often revealing coherent flow structures such as plumes and waves. The observations we present occur in the atmospheric roughness sublayer that is defined to extend from the ground to nearly three times the mean canopy height and is where the presence of the canopy impinges directly on the character of the turbulence [9].

3.1. Wave episodes in CHATS data

Time-lapse animations of more than 1800 hours of high-pass filtered REAL images from the entire CHATS data set were created.¹ The animations of nearly-horizontal scans were carefully examined by the first author for the presence of fine-scale wave packets. A wave packet is distinct from other flow features observed in the lidar images in that the linear bands of enhanced backscatter intensity tend to be oriented perpendicular to the wind direction and the direction in which they propagate. Furthermore, they appear to have a high degree of spatial and temporal coherence compared to plumes and wind parallel streaks sometimes observed during periods of turbulent flow. For a wave packet to be included in this study, it must have passed through the tower (located 1.6 km directly south of the lidar) and have a lifetime longer than one minute. Our subjective judgments of the coherence of the wave packets were based on the clear identification of crests and troughs and movement together as a group. For each case 6 quantities were recorded: date, time when the wave packet forms, time when the packet is no longer coherent, the number of frames that the wave packet is

¹Time-lapse animations are available for viewing at <http://www.phys.csuchico.edu/lidar>

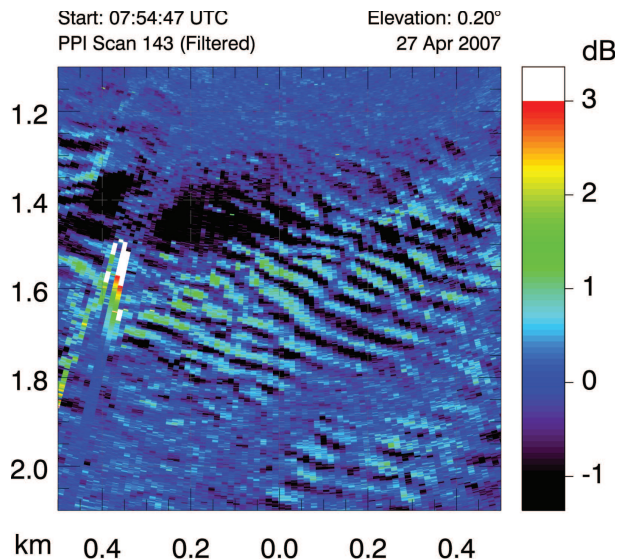


Figure 3: 1 km² section of a single, nearly-horizontal, lidar scan through gravity waves on 27 April 2007 at 7:54 UTC. The wavelength is ~ 70 m. This square area is centered on the location of the tower. The bright marks on the left side are the result of a grove of trees that stood higher than the walnut trees in the orchard. Brighter colors represent higher backscatter intensity.

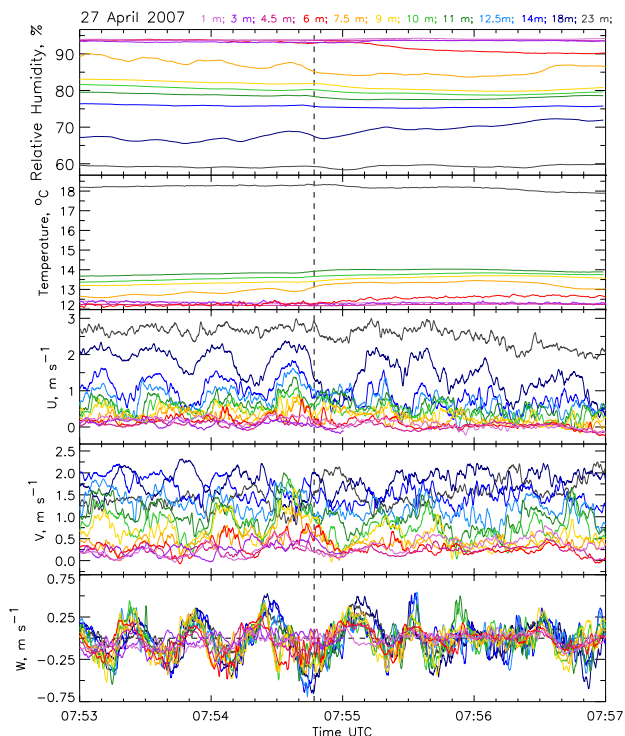


Figure 4: Four minutes of relative humidity, temperature, and three wind components (u , v , and w) time-series data from 12 altitudes on the tower for 27 April 2007 between 7:53 and 7:57 UTC. The wave period is ~ 30 s. The vertical dashed line is placed at the time corresponding to the image in Fig. 3.

visible, the elapsed time between frames, and the average wavelength. Fifty-two wave episodes met the criteria. All cases had one thing in common: none of the wave packets were present during daylight hours. All cases existed between 5:00 and 14:00 UTC, which corresponds to 20 PST to 6 PST. During data collection, the average time of sunset was at 19:44 PST and sunrise at 6:09 PST. In the following section we present three cases selected from the set of 52. They were chosen because of their clarity in both the lidar images and time-series plots.

Figure 3 shows one nearly-horizontal scan from the REAL through a group of waves over the orchard and surrounding the tower on 27 April 2007. At least 12 wave crests and troughs can be identified. Some of these waves are observed over the fields north of the orchard indicating that if the canopy is required for wave formation, they may propagate downstream and over nearby unforested regions. The axes of the crests and troughs are oriented on lines running from approximately the WNW to the ESE. The wavelength is approximately 70 m. The episode lasts 16 minutes. During this time the lidar was collecting such scans at a rate of once per 30 s. Examination of the time-lapse animations clearly suggests the waves are moving from the SW to the NE, however because each wave is similar in shape to the neighboring waves and the significant propagation speed and the relatively low frame rate, it is difficult to estimate wave propagation speed from the animations.

Figure 4 shows time-series from the NCAR ISFF tower that was located 1.6 km directly south of the REAL. The data clearly show evidence of waves in the velocity traces and weakly in the relative humidity trace. The vertical velocity w reveals amplitudes as large as $\pm 0.5 \text{ m s}^{-1}$. The waves have a period of approximately 30 s. By combining the observed wavelength from the lidar (70 m) and the observed period from the in situ sensors (30 s) we obtain a propagation speed of approximately 2.3 m s^{-1} . This is on the same order as the mean wind speed at this time. We also examined the vertical cross-sections (RHI scans) from these periods but were not able to find evidence of the waves in them. This is likely because of the very few number of laser pulses that were projected over such a narrow span of elevation angles and altitudes. In the future, RHI scans can be programmed to reveal the waves in the vertical dimension.

We present two more cases that are similar to 27 April. Figures 5 and 6 show a wave episode on the night of 14 May and Figs. 7 and 8 are from the night of 8 June. The wavelength ($\sim 60\text{--}70 \text{ m}$), orientation (WNW—ESE), period ($\sim 30 \text{ s}$), and structure of the waves in both cases are similar to those observed on 27 April.

4. CONCLUSIONS

The horizontally scanning eye-safe elastic backscatter lidar can identify and confirm the presence of fine-scale gravity waves over forest canopies. The lidar images contain quantitative spatial information such as wavelength that is not available from in situ time-series data. A

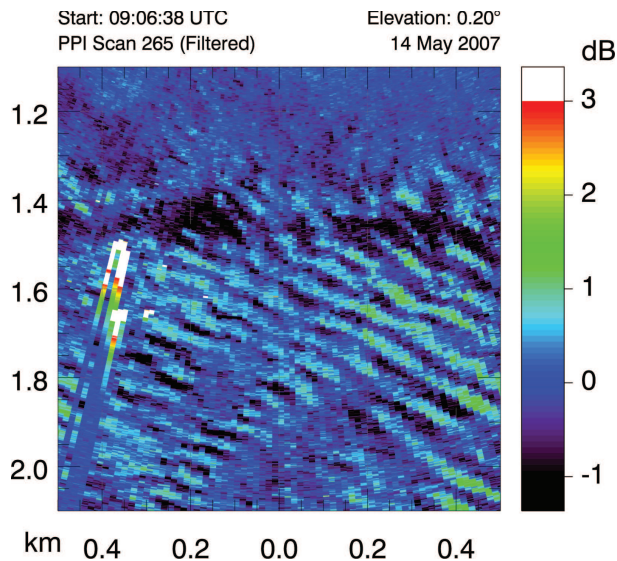


Figure 5: 1 km^2 area of a single, nearly-horizontal, lidar scan through gravity waves on 14 May 2007 at 9:06 UTC. The wavelength is $\sim 70 \text{ m}$. This image is centered over the tower and the in situ data for a 6-minute time span surrounding this image are shown in Fig. 6. The altitude of this cross-section, and those shown in Figs. 3 and 7, is $\sim 18 \text{ m} - 22 \text{ m AGL}$.

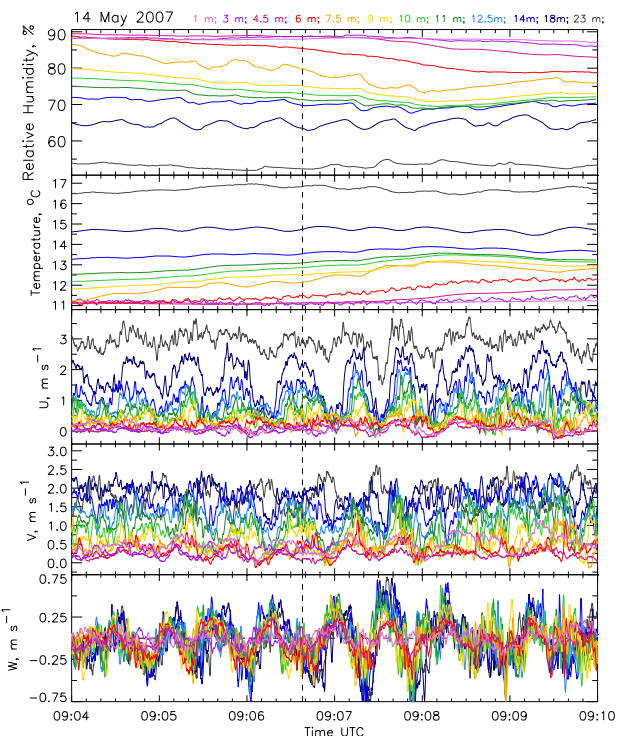


Figure 6: Six minutes of relative humidity, temperature, and three wind component time-series from 12 altitudes on the tower for 14 May 2007 between 9:04 and 9:10 UTC. The vertical dashed line is placed at the time corresponding to the image in Fig. 5

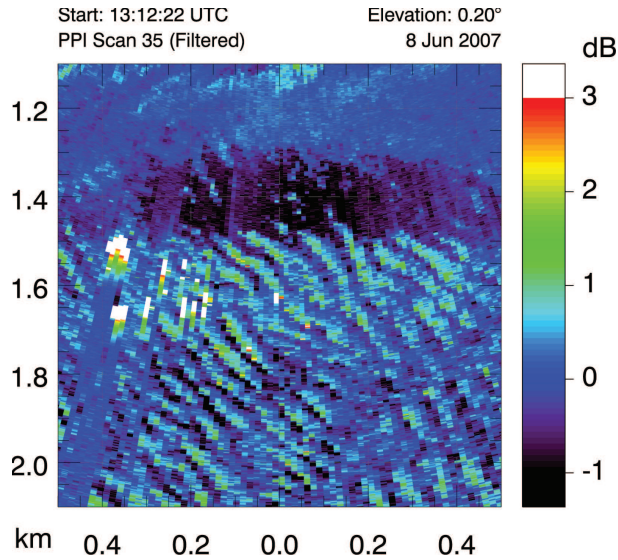


Figure 7: 1 km² area of a single, nearly-horizontal, lidar scan through gravity waves on 8 June 2007 at 13:12 UTC. The wavelength is ~ 60 m. This image is centered over the tower and the in situ data for a 4-minute time span surrounding the time of this image are shown in Fig. 8.

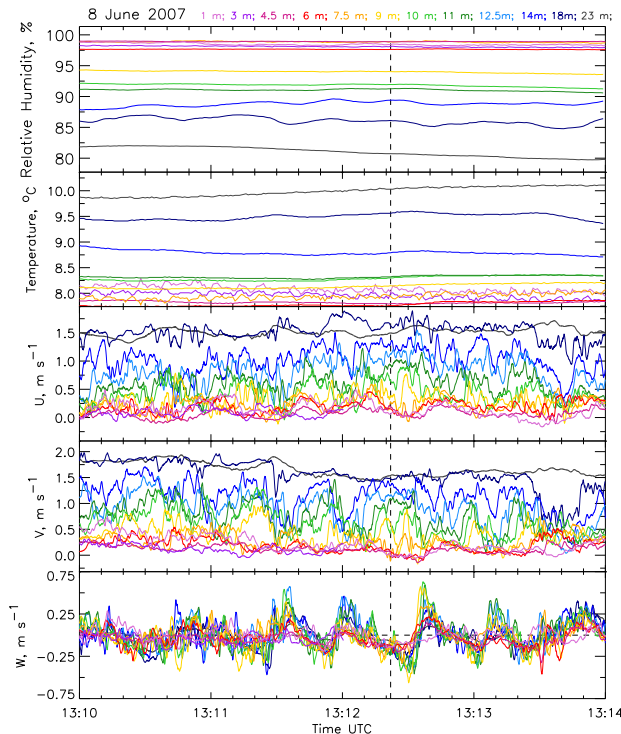


Figure 8: Four minutes of relative humidity, temperature, and three wind component time-series from 12 altitudes on the tower from 8 June 2007 between 13:10 and 13:14 UTC. The vertical dashed line is placed at the time corresponding to the image scan shown in Fig. 7

key requirement for such lidar measurements is high spatial resolution images and sensitivity to small changes in aerosol backscatter. Radial high-pass median filtering is used to clarify the presence of the waves in the images. We note the spacing of backscatter data points in the radial direction of the REAL data is 1.5 m. This enables the instrument to resolve these wave structures that occur on scales of tens of meters.

ACKNOWLEDGMENTS

This paper is based upon research supported by the US National Science Foundation Physical and Dynamic Meteorology program under Grant 0924407.

REFERENCES

1. Stull, R. B. *An Introduction to Boundary Layer Meteorology*. Kluwer Academic Publishers, Dordrecht, The Netherlands, 1988.
2. Cava, D., U. Giostra, M. Siqueira, and G. Katul, 2004: Organised Motion and Radiative Perturbations in the Nocturnal Canopy Sublayer Above an Even-Aged Pine Forest, *Boundary-Layer Meteorol.*, **112**, pp. 129-157.
3. Van Gorsel, E., I. N. Harman, J. J. Finnigan, and R. Leuning, 2011: Decoupling of Air Flow Above and in Plant Canopies and Gravity Waves Affect Micrometeorological Estimates of Net Scalar Exchange, *Agr. Forest Meteorol.*, **151**, pp. 927-933.
4. Lee, X., 1997: Gravity Waves in a Forest: A Linear Analysis, *J. Atmos. Sci.*, **54**, pp. 2574-2585.
5. Lee, X., et al., 1997: Observation of Gravity Waves in a Boreal Forest, *Boundary-Layer Meteorol.*, **84**, pp. 383-398.
6. Fitzjarrald, D. R. and K. E. Moore, 1990: Mechanisms of Nocturnal Exchange between the Rain Forest and the Atmosphere, *J. Geophys. Res.*, **95(D10)**, pp. 16,839-16,850.
7. Patton, E. G., et al., 2011: The Canopy Horizontal Array Turbulence Study (CHATS) *Bull. Amer. Meteorol. Soc.*, **92**, pp. 593-611.
8. Mayor, S. D., S. M. Spuler, B. M. Morley, and E. Loew, 2007: Polarization lidar at 1.54-microns and observations of plumes from aerosol generators, *Opt. Eng.*, **46**, DOI: 10.1117/12.781902.
9. Kaimal, J. C., and J. J. Finnigan, *Atmospheric Boundary Layer Flows: Their Structure and Measurement*. Oxford University Press, Inc., New York, 1994.
10. Lee, X., and A. G. Barr, 1998: Climatology of Gravity Waves in a Forest, *Q. J. Roy. Meteorol. Soc.*, **124**, pp. 1403-1419.
11. Raupach, M. R., and A. S. Thom, 1981: Turbulence in and above Plant Canopies, *Annu. Rev. Fluid Mech.*, **13**, pp. 97-129.
12. Bergström, H. and U. Högström, 1989: Turbulent exchange above a Pine Forest. 2. Organized Structures *Boundary-Layer Meteorol.*, **49**, pp. 231-263.